Inverse Dynamics of a Swimmer Multibody Model: An Analysis of the Upper Limbs During Front Crawl

Francisca Simões

franciscatcsimoes@tecnico.ulisboa.pt

Instituto Superior Técnico, Universidade de Lisboa, Portugal

October 2021

ABSTRACT

The aim of this study is to propose a full-body skeletal model of the human body including a detailed representation of the shoulder complex for the biomechanical analysis and assessment of swimming activities. Considering multibody dynamics, a three-dimensional biomechanical model using Cartesian coordinates is proposed.

Kinematic data were collected at the LABIOMEP-UP for a male swimmer performing a six-beat front crawl swimming technique and the shoulder rhythm was estimated using state of the art regression equations. External forces describing the interaction between the human body and the surrounding environment were estimated using a computer simulation method available in the literature. A determinate inverse dynamic analysis is performed considering the full body biomechanical model actuated upon by driver actuators to evaluate the joint torques and intersegmental joint forces acting on the upper extremity, particularly on the glenohumeral, sternoclavicular and acromioclavicular joints.

The results of the determinate problem are presented and discussed for the anatomical joints of the human upper limbs. The intersegmental forces and joint torques were evaluated for a left-stroke cycle, presenting higher absolute peaks in the most propulsive stages, the insweep and upsweep. The results obtained with a detailed model of the shoulder, considering the clavicle and the scapula, were also compared with a classic model of the shoulder, in which the shoulder joint was modelled as a simple ball-and-socket joint connecting the humerus to the thorax. Overall, the results of the intersegmental forces and joint torques have little or no effect of this increased level of shoulder discretization.

Keywords: Multibody dynamics, Front Crawl Swimming, Hydrodynamic forces, Shoulder complex.

1 INTRODUCTION

In swimming activities, performance enhancement can be analysed within a physiological, biomechanical and fluid dynamics framework. The success of a swimmer is based on several inter-related factors, making it a very complex and challenging field of study for researchers (Barbosa et al., 2011). To realistically analyse and understand the swimming motion, active drag forces, effective propulsive forces, propelling efficiency and power output should be considered (Toussaint & Beek, 1992). These aspects, highly influenced by factors such as the swimming technique, body position, breathing pattern, wall turns and finger spacing, are key to optimize the swimming stroke. Nonetheless, these are very difficult to measure them experimentally and in a non-invasive way (R. C.Z. Cohen et al., 2010; Lauer et al., 2016).

Asides from the motion capture difficulties in an aquatic environment, modelling the front crawl swimming technique has some challenges, for instance, the sudden and high deformations of the swimmer body shape, the complex fluid problem (Cohen et al., 2020) and the asymmetric behaviour of the right and left sides of the human body, either due to the inherently out of phase stroke movement or by the uneven breathing patterns (Psycharakis & Sanders, 2008). Consequently, most studies in the biomechanics of swimming have focused on a single region of the human body (Cohen et al., 2015; Lauer et al., 2016) with largely oversimplified biomechanical models.

During the front crawl swimming motion, the upper body plays a significant role in thrusting, accounting for almost 85% – 90% of total propulsive activity of the swimmer (Guignard et al., 2019; Toussaint & Beek, 1992). However, all biomechanical models applied for swimming activities to the present date neglect the shoulder girdle, limiting their ability to simulate and study the complex shoulder mechanism. The wide range of motion required to perform the front crawl swimming technique is a result of the coordinated interplay between all components of the shoulder complex, including the sternoclavicular, acromioclavicular, glenohumeral and scapulothoracic and joints, all of which are critical for an accurate description of the shoulder biomechanics.

This study proposes a three-dimensional full-body skeletal model of the human body with a detailed representation of the shoulder, based on Quental et al. (2012) to address the shortcomings of current biomechanical models for swimming activities, namely in the evaluation of the internal forces of the upper limbs through inverse dynamics. The shoulder rhythm was estimated using regression equations proposed by Xu et al. (2014) and the external forces acting on the human body during swimming, herein referred to as hydrodynamic forces, were determined using a simulation software available in the literature, the Swimming Human Model with Synthetic User Interface Tools (Swumsuit, Nakashima et al., 2007).

2 METHODS

2.1 Biomechanical Model

The current biomechanical model followed a combination of the works of Oliveira (2016), for a description of the whole body, and Quental et al. (2012), for a more accurate discretization of the upper limb. The model considers 20 rigid bodies including the pelvis, torso, neck, head, and right and left thighs, legs, feet, clavicles, scapulae, arms, forearms, and hands. The body segments are constrained by nineteen anatomical joints: twelve spherical (ball-and-socket) joints, four universal (cardan) joints, and three revolute (hinge) joints. The complete articular system comprises right and left hip, knee, ankle, SC, AC, GH, elbow, and wrist joints and the lumbar, cervical and occipital joints. For the sake of simplicity, the scapulothoracic joints were neglected and the upper extremity was modelled as an open chain.

The computation of the body segment inertial parameters of the biomechanical model follows the dataset of scaling equations proposed by Dumas et al. (2007a, 2007b), except for the head and which are considered two separate bodies, following the approach proposed by Pàmies (2012) – and the shoulder girdle. The kinematic data provided by LABIOMEP-UP are obtained for a 25-year-old male swimmer with 70.3 kg, and 1.80 m. the shoulder girdle was modelled based on the work of Quental et al. (2012), which relied on data computed by Garner & Pandy (2001). To ensure consistency of the shoulder girdle data with the developed biomechanical model, the anthropometric information extracted from the Lisbon Shoulder Model (LSM, Quental et al., 2012) was scaled to match the characteristics computed using the regression equations applied to the subject under analysis (Dumas et al., 2007a, 2007b).

2.2 Shoulder Rhythm Estimation

The dynamic tracking of the scapula and clavicle is very challenging (Grewal & Dickerson, 2013). The most common approach used to capture the shoulder rhythm considers skin markers, but even though three bony landmarks can be identified on the scapula, their tracking is limited due to the relative motion between the bony segment and the overlying soft tissue (Brochard et al., 2011; van Andel et al., 2009; Xu et al., 2014). Predictive statistical models address this challenge, by establishing a consistent correlation between the orientation of the skeletal elements of the shoulder girdle (van der Helm & Pronk, 1995).

The shoulder rhythm proposed by Xu et al. (2014) uses the orientation of humerus relatively to the thorax to predict the orientation of the clavicle and the scapula, offering not only the widest range of motion in the literature but also the greatest angular resolution of all methods to date. These regression equations are represented in generic terms as:

$$\begin{aligned} Y = {} & c_1'(\gamma_{HT1} - 46.97) + c_2'(\beta_{HT} + 66.46) + c_3'(\gamma_{HT2} + 37.64) + c_4'(\gamma_{HT1} - 46.97)^2 \\ & + c_5'(\beta_{HT} + 66.46)^2 + c_6'(\gamma_{HT2} + 37.64)^2 + c_7'(\gamma_{HT1} - 46.9)(\beta_{\mathrm{HT}} + 66.46) \\ & + c_8'(\gamma_{\mathrm{HT1}} - 46.97)(\gamma_{\mathrm{HT2}} + 37.64) + c_9'(\beta_{\mathrm{HT}} + 66.46)(\gamma_{\mathrm{HT2}} + 37.64) + \mathrm{K} \end{aligned} \quad (1)$$

with c_i', γ_{HT1}, β_{HT}, γ_{HT2}, and K, representing the estimated regression coefficients, the angle of the humerothoracic plane of elevation, the humerothoracic angle of elevation, the angle of axial rotation, and a given constant, respectively. The regression coefficients c_i' are detailed in Table XX for the retraction/protraction of the scapula ($\boldsymbol{\gamma_S}$), lateral/medial rotation of the scapula (β_S), anterior/posterior tilt of the scapula (α_S), retraction/protraction of the clavicle (γ_C), and elevation/depression of the clavicle (β_C).

Table 1: Estimated regression coefficients for the predictive equations from Xu et al. (2014)

$\boldsymbol{Y}$	$\boldsymbol{c_1'}$	$\boldsymbol{c_2'}$	$\boldsymbol{c_3'}$	$\boldsymbol{c_4'}$	$\boldsymbol{c_5'}$	$\boldsymbol{c_6'}$	$\boldsymbol{c_7'}$	$\boldsymbol{c_8'}$	$\boldsymbol{c_9'}$	$\boldsymbol{K}$
$\boldsymbol{\gamma_S}$	0.163	-	0.039	-0.0016	-0.0018	-0,0003	-0.0023	-0.0009	0.0003	38.35
$\boldsymbol{\beta_S}$	-0.065	0.322	-0.024	-	-0.0009	-	-	-0.0014	-	-23.20
$\boldsymbol{\alpha_S}$	0.060	-0.039	-0.011	-	-	0.0002	-	0.0005	0.0008	-7.11
$\boldsymbol{\gamma_C}$	0.059	0.207	0.013	-0,0017	-0.0005	-0.0005	-0.0020	-0.0020	-	-17.42
$\boldsymbol{\beta_C}$	-0.025	0.204	-0.031	-	0.0002	0.0002	-0.0007	-0.0003	0.0007	-21.04

2.3 Kinematic Consistency

The experimental data collected at the LABIOMEP-UP involved a 25-year-old healthy male swimmer with a height of 1.80 m and a weight of 70.3 kg. The athlete performed a front crawl swimming stroke for the purpose of data graphic visualization in a 25m indoor swimming pool, i.e., motion was acquired to recreate the front crawl swimming motion through video imaging. Considering a Cartesian coordinates formulation, the body-fixed, or local, reference frame of each body segment is defined following the recommendations of the *International Society of Biomechanics* (ISB) (Wu et al., 2002, 2005). After proper filtering of the kinematic data to remove noise, a kinematic analysis is performed to ensure the calculation of consistent positions, velocities, and accelerations between both laboratorial and model data (Silva and Ambrósio, 2002).

2.4 Estimation of the Hydrodynamic Forces

In this work, the external forces that were applied on the swimmer's biomechanical model, i.e., the hydrodynamic forces, were estimated using Swumsuit, the simulation software developed by Nakashima et al. (2007). The interface developed by Sequeira (2021) was used to convert the results obtained after a kinematic consistency analysis into suitable inputs for Swumsuit and to convert the software's outputs into adequate kinetic data developed for the actual swimming motion, necessary for the inverse dynamic analysis.

2.4.1 Interface between Swumsuit and Current Model

Swumsuit requires four types of input files to estimate the hydrodynamic forces: 1) the body geometry data file, with information about the swimmer's body topology and anthropometric characteristics; 2) the joint motion data file, describing the orientation of all anatomical segments during the complete stroke cycle; 3) the linear and angular velocities data file, reporting the linear and angular velocities of the swimmer's body all a whole and 4) the analysis settings data file, with information about the analysis parameters and the system's initial conditions.

Since the SWUM model and the current biomechanical model have different discretization levels, a relationship had to be established between the two. Sequeira (2021) defined a relationship between a biomechanical model composed of 16 rigid bodies (with a direct correspondence to the current model except for bodies 17-20, right and left clavicles and right and left scapulae) and the SWUM model, composed of 21 rigid bodies. For the sake of simplicity, this work follows the same equivalence defined by Sequeira (2021) and assumes the right and left clavicles and scapulae have no direct forces applied.

2.4.2 Joint Motion Reconstruction

The angular conversion methodology proposed by Sequeira (2021) included a segment-specific approach, i.e., not all the body had their rotations converted with the same sequence, nor had the same number of rotations. To address these limitations, a more robust and standardized procedure to convert Euler parameters to Euler angles is proposed here.

Swumsuit defines each rotation relatively to a reference frame that is fixed on the proximal joint before the movement starts. Moreover, SWUM rotations are defined sequentially, based on two chains: the upper and the lower chain. These two chains are ordered from proximal to distal segments and are linked to one another at the whole-body centre of mass (COM), which is located at the lower tip of the lower waist segment (Nakashima et al., 2007). The upper chain (UC) begins at the lower waist segment and connects all the bodies until the extremities located of the upper body – head and right and left hands. Analogously, the lower chain (LC) is defined from the upper hip all the way down to the feet.

To define a robust and systematic transformation of the four Euler parameters, obtained after ensuring kinematic consistency, into rotation angles, the following procedure was developed. The orientation of each SWUM body segment is calculated in the global reference frame of Swumsuit, $\mathbf{R}_{\mathrm{SWUM}}$:

$$(\mathbf{R}_{\mathrm{SWUM}})_i = (\mathbf{R}_{\mathrm{Model}})_j \times (\mathbf{R}_{\mathrm{SWUM2Model}})_i \quad (2)$$

where $\mathbf{R}_{\mathrm{Model}}$ represents the orientation of each body j in the global reference frame of the current model, calculated by directly converting Euler parameters into their corresponding rotation matrix, and $\mathbf{R}_{\mathrm{SWUM2Model}}$ represents the orientation of the SWUM body j defined in the body-fixed reference frame of the corresponding body in the current model. These matrices are computed by establishing an initial rotation matrix that relates the orientation of each body-fixed coordinate system in SWUM with the local

frame of each corresponding body j in the current model, both of them in the reference position, with the upper limbs raised upwards, the trunk and lower limbs straight, and the feet pointing downwards. Each SWUM joint allows 3 rotational DOF defined relatively to its predecessor body, bearing in mind the above defined UC and LC. For the purpose of this joint motion reconstruction methodology, all rotations are assumed to occur sequentially and in the same order ZYX.

2.5 Inverse Dynamic Analysis

In an inverse dynamic analysis, in which the kinematic data are fully known, the equations of motion are solved for the unknown Lagrange multipliers, which are directly associated with the intersegmental joint forces and joint torques of the human body model (Silva and Ambrósio, 2003). This Lagrange multipliers quantify the intersegmental forces that are developed by the kinematic constraints. An inverse dynamic analysis is performed in MATLAB (Mathworks, Natick, MA) considering a fully determined problem, in which the DOF of the biomechanical model are actuated by driver actuators. The equations of motion are given by:

$$\mathbf{M}\ddot{\mathbf{q}} + \boldsymbol{\Phi}_{\mathbf{q}}^{\mathrm{T}}\boldsymbol{\lambda} = \mathbf{g} \tag{1}$$

where $\mathbf{M}$ is the global mass matrix of the system, $\ddot{\mathbf{q}}$ is the vector of global consistent accelerations, $\boldsymbol{\Phi}_{\mathbf{q}}^{\mathrm{T}}$ is the Jacobian matrix, $\boldsymbol{\lambda}$ is the vector of Lagrange multipliers associated with the intersegmental forces developed by the kinematic constraints, and $\mathbf{g}$ is the vector of externally applied forces.

3 RESULTS AND DISCUSSION

The solution of the determinate inverse dynamics analysis is shown and discussed here. The intersegmental joint torques that are responsible for the movements in the sagittal, transverse and frontal planes obtained during the six-beat front crawl swimming motion are depicted in Figure 1 and **Error! Reference source not found.** for the right shoulder and the right sternoclavicular and right acromioclavicular joints, respectively. Figure 1 also illustrates a comparison between the results obtained for a classic shoulder model are compared with those of the detailed shoulder model. The classic shoulder approach models the shoulder joint simply as a spherical joint that connects the humerus to the thorax, whereas the detailed shoulder model considers the clavicle and the scapula. This second approach, despite not representing the closed loop chain, includes the AC joint, connecting the scapula and the clavicle, the SC joint, linking the clavicle and the sternum, and the glenohumeral joint (shoulder joint), here coupling the humerus to the scapula. Modelling the shoulder girdle in a more discretized manner allows a better, more accurate representation of the shoulder rhythm, which can be seen as a clear advantage to understand the shoulder behaviour in the swimming context.

Resultant joint torques are also obtained during a left-hand six-beat front crawl swimming stroke cycle in the right shoulder, elbow and wrist, and are represented in Figure 3. The resultant torque peaks and average values are shown in Table 2.

(a)

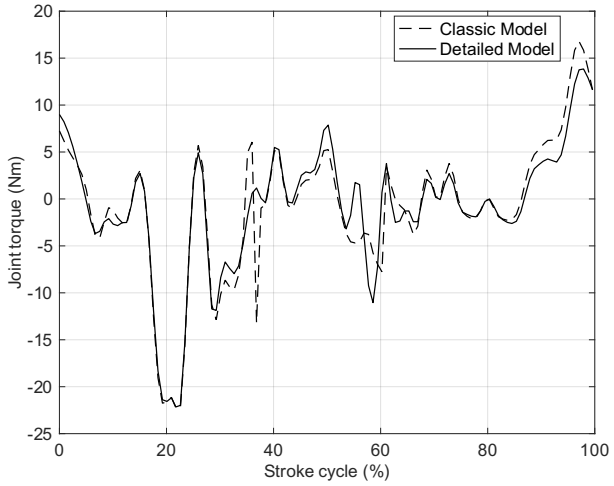

(b)

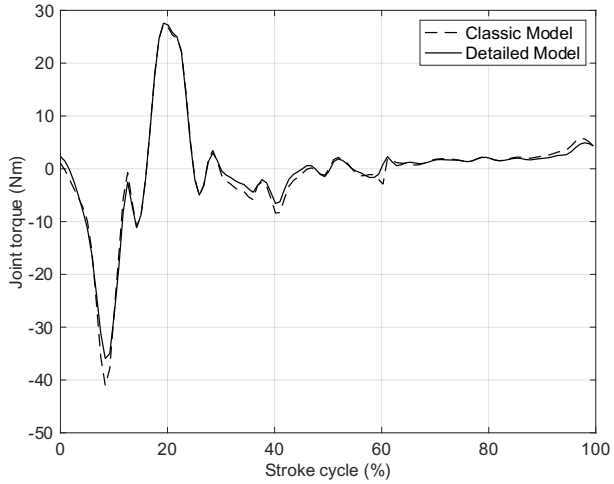

(c)

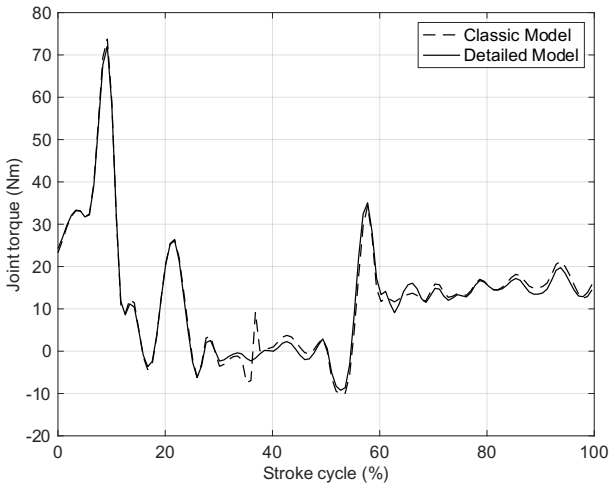

Figure 1: Joint torques obtained during left-hand six-beat front crawl swimming stroke cycle for the right shoulder. The represented joint torques are responsible for the right shoulder movements in the a) sagittal, b) transverse and c) frontal planes.

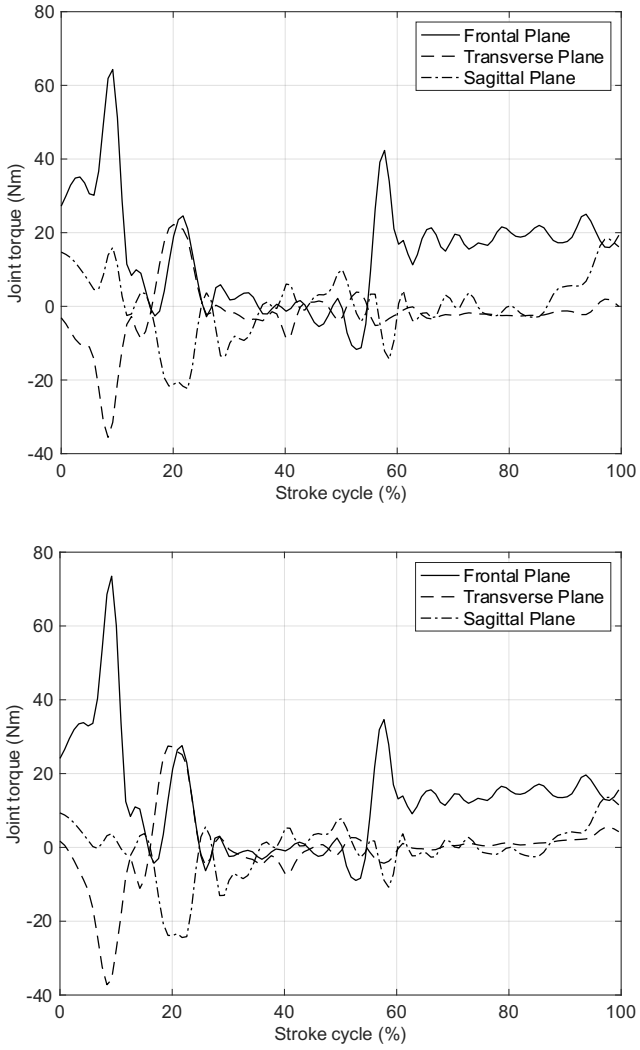

Figure 2: Joint torques obtained during left-hand six-beat front crawl swimming stroke cycle in the right a) sternoclavicular b) acromioclavicular.

During the entry and stretch stage (54%-58%), the swimmer sets up the arm and body to produce as much thrust as possible: the body roll begins at hand entry, the glenohumeral joint is marginally externally rotated and abducted, which is confirmed by the negative joint torque value inducing the movement in both transverse and frontal planes (Figure 1). The scapula starts abducted but soon adducts and rotates downward. Throughout the downsweep (58%-100%; 0%-9%), the glenohumeral joint flexes and the body rolls, partially promoted by the shoulder roll; at the end of this phase, the glenohumeral joint starts adducting, which is supported by the valley of about -35 Nm (detailed shoulder model) found in the first instants of the left stroke cycle pictured in Figure 1. During the insweep phase (9%-18%), when the upper limb does most of the work in propelling the body forward using the resistance of the water, the glenohumeral joint is adducted, internally rotated, and extended. The upsweep stage (18%-28%) contemplates the glenohumeral movement of extension, adduction and internal rotation in the sagittal, frontal and transverse planes; assuming that the scapular plane is aligned with the frontal plane, the scapula denotes a downward movement of rotation and adduction, confirmed by the AC joint torques that induce the motion in the transverse plane (always positive, achieving a peak at 28 Nm) and in frontal plane (predominantly positive, reaching a peak of about 28 Nm). At the end of this phase, the body

progressively returns to the horizontal swimming position with the arm close to the water surface. The final stage of the stroke, the recovery phase (28%-54%), is conducted above the water. The arm movement is induced by a slight glenohumeral abduction and external rotation, as evidenced by the -5 Nm (maximum abduction moment in this period) and -9 Nm (maximum external rotation moment in recovery). In the beginning of the recovery phase, the elbow extends, and the scapula rotates downward and adducts. From mid-recovery until the end of the cycle, the glenohumeral joint continues to be externally rotated beyond the neutral position and slightly abducts, achieving its maximum relative abduction right before the hand entering the water for another cycle; the scapula protracts and rotates upward. Right at the end of the recovery, the body returns to the fully horizontal swimming position and is ready to initiate the next stroke.

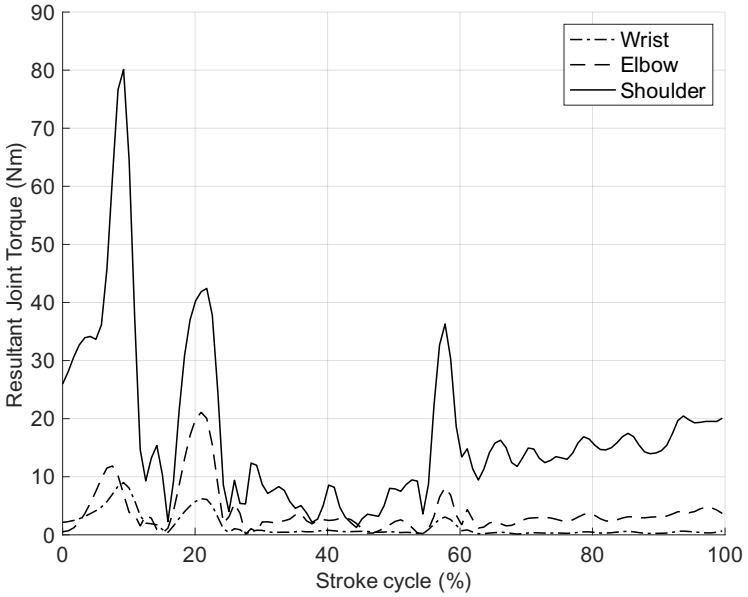

Figure 3: Resultant joint torques obtained during left-hand six-beat front crawl swimming stroke cycle in the right shoulder, elbow and wrist. The dot-dashed line depicts the resultant joint torque profile for the wrist joint, the dashed line represents the results obtained for the elbow, and the continuous line embodies the results achieved by the shoulder joint.

The resultant torque is approximately zero during the recovery phase and vestigial in the entry phase. The largest peaks are consistently detected in the wrist, elbow and shoulder joints and occur approximately at the end of the downsweep stage (during the pull) and in the mid-push phase (at the end of the insweep and in the beginning of the upsweep), overall agreeing with the results found by Harrison et al. (2014). However, a significant difference is found in the magnitude of the resultant torques when comparing the results of the present work and to those obtained by Harrison et al. (2014), shown in Table 2:

Table 2: Comparison between the average and peak magnitudes of resultant joint torques of the wrist, elbow and shoulder obtained in the current work versus the results from Harrison et al. (2014).

	Average Resultant Torque (Nm)		**Peak Resultant Torque** (Nm)	
	Current model	Harrison et al. (2014)	Current model	Harrison et al. (2014)
Wrist	1.4	5	9	17
Elbow	3.9	21	21	85
Shoulder	17.4	43	80	176

4 CONCLUSIONS AND FUTURE WORK

The results of the inverse dynamic analysis were discussed for the principal articulations responsible for the motion of the human upper limbs, namely the right wrist, elbow and the shoulder complex joints: glenohumeral, sternoclavicular and acromioclavicular. All joints are thought to show agreement with the expected variation from positive to negative values during the different swimming stages. Predictably, the most propulsive stages, namely the insweep and upsweep, are responsible for the higher demanding efforts.

For a determinate inverse dynamic analysis, the effect of having the shoulder rhythm described as the coordinated action of the GH, SC and AC joints shows little to no influence in the behaviour of the glenohumeral joint, when compared to the shoulder joint of the classic model. A possible explanation for this could be the fact that, although connecting different bodies, depending on the model, the centre of rotation of the glenohumeral/shoulder joint remains approximately in the same location. This situation, allied to the fact that the kinematics of the arm is kept unchanged between the two models and that the clavicle and scapula have no applied external forces, leads to similar joint torques.

From the biomechanical modelling point of view, a more realistic discretization of the shoulder complex should be considered. The current model includes the glenohumeral, sternoclavicular and acromioclavicular joints, neglecting the effect of a fourth pseudo-joint, the scapulothoracic joint, which represents the sliding behaviour of the scapula over the thoracic wall. Often modelled by two holonomic constraints (Quental et al., 2012), this pseudo articulation closes an otherwise open-chain shoulder mechanism, being fundamental to established a more realistic force equilibrium, naturally affecting the joint reaction torques or, in the case of a muscle force sharing problem, the muscle actuators.

To address the shortcomings of the kinematic and kinetic acquisitions in water settings, an integrated approach considering shoulder rhythm predictive equations developed by Xu et al. (2014), kinematic data processing and subsequential estimation of the hydrodynamic forces using the simulation software Swumsuit (Nakashima et al., 2007), was considered. The regression equations proposed by Xu et al. (2014) do not cover the entire range of motion of the shoulder in the context of swimming, so they extrapolated the shoulder rhythm in this work. Therefore, future studies on the shoulder rhythm during swimming should be based on either adequate protocol to measure the shoulder kinematics or rely on regression equations with that cover wider ranges of motion.

The computed intersegmental joint forces do not have physiological meaning and the joint reaction torques do not directly predict magnitudes of muscle forces. Future works should incorporate muscle models to calculate muscle, tendon, and actual joint reaction forces. Additionally, a musculoskeletal model of upper limb may be crucial to realistically analyse the impact of having a detailed versus a classic shoulder model during the study of not only the front crawl, but also of other techniques such as the breaststroke, butterfly and back strokes.

References

Barbosa, T. M., Marinho, D. A., Costa, M. J., & Silva, A. J. (2011). Biomechanics of Competitive Swimming Strokes. In V. Klika (Ed.), *Biomechanics in Applications*. IntechOpen. https://doi.org/10.5772/19553

Cohen, R. C.Z., Cleary, P. W., & Mason, B. (2010). Improving understanding of human swimming using smoothed particle hydrodynamics. *IFMBE Proceedings*, *31 IFMBE*, 174–177. https://doi.org/10.1007/978-3-642-14515-5_45

Cohen, R. C.Z., Cleary, P. W., Mason, B. R., & Pease, D. L. (2020). Studying the effects of asymmetry on freestyle swimming using smoothed particle hydrodynamics. *Computer Methods in Biomechanics and Biomedical Engineering*, *23*(7), 271–284. https://doi.org/10.1080/10255842.2020.1718663

Dumas, R., Chèze, L., & Verriest, J. P. (2007a). Adjustments to McConville et al. and Young et al. body segment inertial parameters. *Journal of Biomechanics*, *40*(3), 543–553. https://doi.org/10.1016/j.jbiomech.2006.02.013

Dumas, R., Chèze, L., & Verriest, J. P. (2007b). Corrigendum to "Adjustments to McConville et al. and Young et al. body segment inertial parameters" [J. Biomech. 40 (2007) 543-553]. *Journal of Biomechanics*, *40*(7), 1651–1652. https://doi.org/10.1016/j.jbiomech.2006.07.016

Guignard, B., Chollet, D., Vedova, D. D., Rouard, A., Bonifazi, M., Hart, J., & Seifert, L. (2019). Upper to lower limb coordination dynamics in swimming depending on swimming speed and aquatic environment manipulations. *Motor Control*, *23*(3), 418–442. https://doi.org/10.1123/mc.2018-0026

Harrison, S. M., Cohen, R. C. Z., Cleary, P. W., Mason, B. R., & Pease, D. L. (2014). Torque and power about the joints of the arm during the freestyle stroke. *12th International Symposium on Biomechanics and Medicine in Swimming*, *January*, 349–355.

Lauer, J., Rouard, A. H., & Vilas-Boas, J. P. (2016). Upper limb joint forces and moments during underwater cyclical movements. *Journal of Biomechanics*, *49*(14), 3355–3361. https://doi.org/10.1016/j.jbiomech.2016.08.027

Nakashima, Motomu, Satou, K., & Miura, Y. (2007). Development of Swimming Human Simulation Model Considering Rigid Body Dynamics and Unsteady Fluid Force for Whole Body. *Journal of Fluid Science and Technology*, *2*(1), 56–67. https://doi.org/10.1299/jfst.2.56

Quental, C., Folgado, J., Ambrósio, J., & Monteiro, J. (2012). A multibody biomechanical model of the upper limb including the shoulder girdle. *Multibody System Dynamics*, *28*(1–2), 83–108. https://doi.org/10.1007/s11044-011-9297-0

Sequeira, M. (2021). *Inverse Dynamics of a Swimmer Multibody Model : An Analysis of the Lower Limbs During Front Crawl* (Issue January). University of Lisbon.

Silva, M. P. T., & Ambrósio, J. A. C. (2002). Kinematic data consistency in the inverse dynamic analysis of biomechanical systems. *Multibody System Dynamics*, *8*(2), 219–239. https://doi.org/10.1023/A:1019545530737

Toussaint, H. M., & Beek, P. J. (1992). Biomechanics of Competitive Front Crawl Swimming. *Sports Medicine: An International Journal of Applied Medicine and Science in Sport and Exercise*, *13*(1), 8–24. https://doi.org/10.2165/00007256-199213010-00002

van der Helm, F. C. T., & Pronk, G. M. (1995). Three-Dimensional Recording and Description of Motions of the Shoulder Mechanism. *Journal of Biomechanical Engineering*, *117*, 27–40. http://biomechanical.asmedigitalcollection.asme.org/

Wu, G., Siegler, S., Allard, P., Kirtley, C., Leardini, A., Rosenbaum, D., Whittle, M., D'Lima, D., Christofolini, L., Witte, H., Schmid, O., & Stokes, I. (2002). ISB recommendation on definitions of joint coordinate system of various joints for the reporting of human joint motion—part I: ankle, hip, and spine. *Journal of Biomechanics*, *35*(2), 543–548.

Wu, G., Van Der Helm, F. C. T., Veeger, H. E. J., Makhsous, M., Van Roy, P., Anglin, C., Nagels, J., Karduna, A. R., McQuade, K., Wang, X., Werner, F. W., & Buchholz, B. (2005). ISB recommendation on definitions of joint coordinate systems of various joints for the reporting of human joint motion - Part II: Shoulder, elbow, wrist and hand. *Journal of Biomechanics*, *38*(5), 981–992. https://doi.org/10.1016/j.jbiomech.2004.05.042

Xu, X., Lin, J. hua, & McGorry, R. W. (2014). A regression-based 3-D shoulder rhythm. *Journal of Biomechanics*, *47*(5), 1206–1210. https://doi.org/10.1016/j.jbiomech.2014.01.043